Probabilistic Multilocus Haplotype Reconstruction in Outcrossing Tetraploids

Chaozhi Zheng,*,[1] Roeland E. Voorrips,[†] Johannes Jansen,* Christine A. Hackett,[‡] Julie Ho,[§] and Marco C. A. M. Bink*

*Biometris and [†]Plant Breeding, Wageningen University and Research Centre, 6708 PB Wageningen, Netherlands, [‡]Biomathematics and Statistics Scotland, Dundee DD2 5DA, Scotland, and [§]Forage Genetics International, Inc., Davis, California 95618-0505

ABSTRACT For both plant (*e.g.*, potato) and animal (*e.g.*, salmon) species, unveiling the genetic architecture of complex traits is key to the genetic improvement of polyploids in agriculture. F_1 progenies of a biparental cross are often used for quantitative trait loci (QTL) mapping in outcrossing polyploids, where haplotype reconstruction by identifying the parental origins of marker alleles is necessary. In this paper, we build a novel and integrated statistical framework for multilocus haplotype reconstruction in a full-sib tetraploid family from biallelic marker dosage data collected from single-nucleotide polymorphism (SNP) arrays or next-generation sequencing technology given a genetic linkage map. Compared to diploids, in tetraploids, additional complexity needs to be addressed, including double reduction and possible preferential pairing of chromosomes. We divide haplotype reconstruction into two stages: parental linkage phasing for reconstructing the most probable parental haplotypes and ancestral inference for probabilistically reconstructing the offspring haplotypes conditional on the reconstructed parental haplotypes. The simulation studies and the application to real data from potato show that the parental linkage phasing is robust to, and that the subsequent ancestral inference is accurate for, complex chromosome pairing behaviors during meiosis, various marker segregation types, erroneous genetic maps except for long-range disturbances of marker ordering, various amounts of offspring dosage errors (up to ~20%), and various fractions of missing data in parents and offspring dosages.

KEYWORDS polyploidy; outbred population; double reduction; preferential pairing; ancestral inference

POLYPLOIDY occurs in some animals such as salmon but is pervasive in plants, including many important crop species such as potato (*Solanum tuberosum*) and alfalfa (*Medicago sativa*). Understanding the genetic architecture of complex traits in polyploids plays a fundamental role in their genetic improvement. Numerous statistical methods have been developed for quantitative trait locus mapping in humans, animal, and plant species with diploid genomes. In contrast, corresponding studies in polyploids are very few, although an analogous linear model framework was introduced for tetraploid mapping populations at least 15 years ago (Xie and Xu 2000; Hackett *et al.* 2001).

In the linear (mixed) models for quantitative trait locus mapping in diploid and polyploid species, the genetic component of a quantitative trait requires the calculation of genetic predictors (covariates), often expressed as the probabilities that the alleles at putative quantitative trait loci (QTL) are derived from particular parental chromosomes conditional on the observed genotypic data of mapping individuals and their parents. The haplotype reconstruction for calculating genetic predictors in diploids has been well developed (Mott *et al.* 2000; Broman *et al.* 2003; Liu *et al.* 2010; Zheng *et al.* 2015). The aim of this work is haplotype reconstruction in a full-sib tetraploid family.

Compared to diploids, there are several challenges for haplotype reconstruction in polyploids. First, traditional marker systems such as dominant amplified fragment length polymorphism (AFLP) and codominant simple sequence repea (SSR) do not provide full information for a straightforward estimation of the number of copies of each allele (dosage). This is so because each score (gel band pattern) may correspond to multiple allelic dosages, and some alleles may not be revealed in a gel band pattern (the null alleles). However, new

doi: 10.1534/genetics.115.185579
Manuscript received December 2, 2015; accepted for publication February 22, 2016; published Early Online February 24, 2016.
Supplemental material is available online at www.genetics.org/lookup/suppl/doi:10.1534/genetics.115.185579/-/DC1.
[1]Corresponding author: Biometris, Wageningen University and Research Centre, P.O. Box 16, 6700 AA Wageningen, Netherlands. E-mail: chaozhi.zheng@wur.nl

genotyping technologies, *e.g.*, the Illumina Infinium platform and sequencing-based methods such as genotyping-by-sequencing, allow accurate estimation of the dosage of high-density single-nucleotide polymorphisms (SNPs) throughout the genome (Voorrips *et al.* 2011; Garcia *et al.* 2013; Hackett *et al.* 2013; Li *et al.* 2014). We focus on analyzing the increasingly available SNP dosage data.

Second, the pairing and segregation of chromosomes during meiosis are more complex in polyploids than in diploids. Polyploids are traditionally classified into allopolyploids and autopolyploids. Allopolyploids are derived from hybridization of two different species and subsequent chromosome doubling, and thus homologous chromosomes are more likely to pair together than homeologous chromosomes (Sybenga 1994). However, in autopolyploids, all the homologous chromosomes can pair during meiosis and form either random (nonpreferential) bivalents or multivalents, leading to polysomic inheritance. To maximize flexibility, we do not make a strict distinction between allopolyploids and autopolyploids, so both preferential bivalent pairing and quadrivalent pairing are possible *a priori* in tetraploids. Quadrivalent pairing can lead to a phenomenon called *double reduction*; *i.e.*, corresponding parts of two sister chromatids of a chromosome sort into the same gamete (Mather 1936).

Last but not least, the parents of a mapping population are often outbred (not homozygous), which requires the crucial reconstruction of parental linkage phases across all SNP markers within each linkage group. For traditional marker systems such as AFLP and SSR in a full-sib tetraploid family, Luo *et al.* (2001) developed a general expectation-maximization algorithm to obtain the most likely phases for all pairs of markers and then reconstructed the phase of the complete linkage group using a heuristic algorithm. This procedure was extended to analyze SNP dosage data (Hackett *et al.* 2013). However, this still requires manual assignment of some SNP marker phases, and its application to large data sets may be slow.

Our approach to haplotype reconstruction in outcrossing tetraploids consists of multilocus parental linkage phasing and subsequent ancestral inference from SNP dosage data. It builds on an integrated network modeling of tetraploid inheritance, accounting for preferential bivalent and quadrivalent pairing. The multilocus linkage phasing is an automatic marker analysis involving no manual manipulation of intermediate results. Conditional on the estimated parental linkage phases, ancestral inference is performed to calculate posterior genotype probabilities at all marker locations based on a hidden Markov model (HMM) derived from the network model. Hackett *et al.* (2013) developed a similar HMM, except that their model assumes bivalent pairing and does not account for quadrivalent pairing. Leach *et al.* (2010) developed multilocus autotetrasomic linkage analysis using a HMM for traditional AFLP and SSR marker data conditional on marker ordering and parental linkage phases; their method accounts for a mixture of random bivalent and quadrivalent pairing, and it also may be used for ancestral inference in autotetraploids.

We assume a given genetic linkage map, *i.e.*, the ordering of SNP markers and the intermarker genetic distances, that may be constructed from two-locus linkage analysis (Luo *et al.* 2001, 2006; Hackett *et al.* 2013). Specifically, for each linkage group, the two-locus analysis produces the recombination fraction and the LOD score for all pairs of markers, which can be used to construct the map using, *e.g.*, the least-squares procedure implemented in JoinMap software (Stam 1993).

To evaluate the robustness of our new haplotype reconstruction method called *TetraOrigin*, we simulate many scenarios, including various chromosome pairing behaviors, various marker segregation types, and erroneous genetic linkage maps. We also study the impact of missing dosage data among parents and offspring and the effects of errors in offspring dosage data. Then we apply TetraOrigin to real potato data (Hackett *et al.* 2013). For both simulation studies and application to real data, we compare TetraOrigin with the methodology described in Hackett *et al.* (2013), henceforth abbreviated to H2013.

Methods

The model overview

Consider a full-sib tetraploid family with two parents denoted P_1 and P_2. We model the genetic inheritance independently across linkage groups and thus consider only one group. We label the four homologous or homeologous chromosomes of parent P_1 1, 2, 3, and 4, assuming that chromosomes *I* and *II* are homologous and that so are chromosomes *III* and *IV*. The four chromosomes of parent P_2 are similarly labeled 5, 6, 7, and 8. The ordering of the two parents and the ordering of the four chromosomes within a parent are otherwise arbitrary. Denote by D_t^o the dosage of offspring $o = 1, \ldots, N_o$ at locus $t = 1, \ldots, N_t$ and D_t^p the dosage of parent $p = P_1, P_2$ at locus t. The ordering and genetic locations of markers are assumed to be known, and all the markers are biallelic.

An overview of the model for analyzing dosage data D_t^o and D_t^p is shown in Figure 1. The offspring dosage data D_t^o are not independent across offspring, which provides information on estimating the parental haplotype $H = \{H_t\}_{t=1}^{N_t}$. Given the parental haplotype and offspring o, the dosage data D_t^o are not independent across markers, which provides information on estimating the chromosome pairing V_o when producing offspring o. Denote this by $V = \{V_o\}_{o=1}^{N_o}$.

Conditional on the parental haplotype H and the chromosome pairing V_o, we model parental origins X_t^o along the four chromosomes of offspring o by a discrete-time Markov chain. The Markov chain can be described by an initial distribution $\pi_j^o = P(X_1^o = j) = 1/N_s$ specifying the probability that the parental origin X_1^o at the first locus is at the jth state for $j = 1, \ldots, N_s$ and an $N_s \times N_s$ transition probability matrix $T^o(t)$ specifying how the parental origin state changes from locus t into the next. The state space of the Markov chain depends on the chromosome pairing V_o, which will be described in the following gamete and zygote models. For convenience, we specify X_t^o, H_t, and V_o by either their discrete values or integer labels starting from 1.

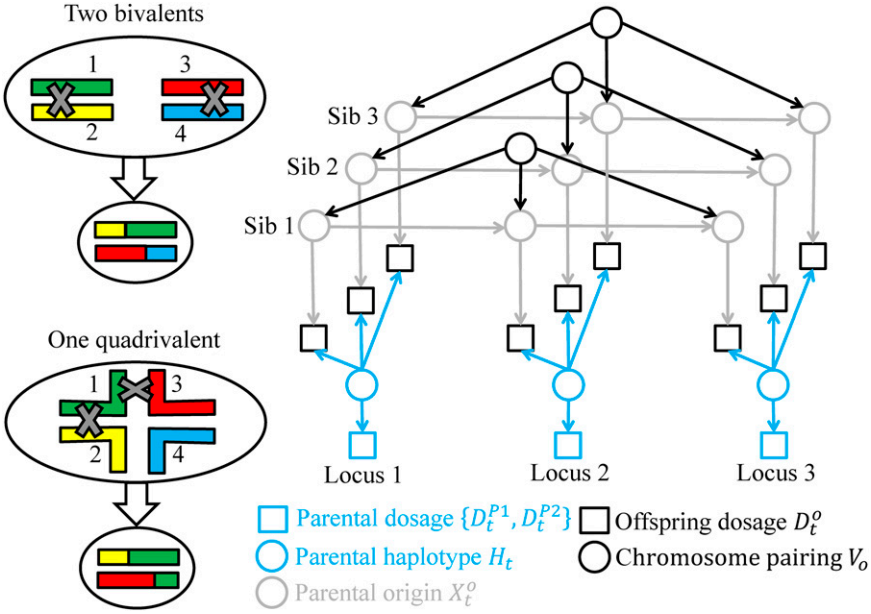

Figure 1 The network model. Left panels refer to the possible gametes produced by either bivalent pairing or quadrivalent pairing in parent P_1, where the four homologous/homeologous chromosomes are labeled by different colors. The right panel refers to the directed acyclic graph of the model for $N_o = 3$ offspring at $N_t = 3$ marker loci, where the rectangles denote known dosage data, the circles random variables, and the solid arrows probabilistic relationships described in the *Methods* section. Conditional on the chromosome pairings $V = \{V_o\}_{o=1}^{N_o}$, the network model becomes a HMM along the chromosomes with the latent variables being the parental haplotypes $\{H_t\}_{t=1}^{N_t}$ and the parental origins $\{X_t^o\}_{t=1,\ldots,N_t}^{o=1,\ldots,N_o}$.

The data likelihood

We first consider that there is no error and no missing data in the parental dosages. At a given locus t, the posterior probability $P(H_t|D_t^{P_1}, D_t^{P_2}) = 1/M_t$ follows a discrete uniform distribution over all possible M_t combinations of haplotypes compatible with parental dosages. For example, the dosages for parents P_1 and P_2 are 1 and 2, respectively. Then there are four possible haplotypes for P_1, 1000, 0100, 0010, and 0001, and six possible haplotypes for P_2, 1100, 1010, 1001, 0110, 0101, and 0011, where we denote by 0 and 1 the two alleles at the locus, and the dosage refers to the number of copies of allele 1. Thus, H_t at this locus is one of the $M_t = 24$ possible combinations, *e.g.*, $(1000,\ 1100)$, at equal probability.

If a parent dosage is missing, we treat all five dosages as equally probable with probability 1/5. When modeling errors are seen in the parent dosages, we assume that each observed dosage is the true dosage with probability $1 - \varepsilon_F$ and that all the other four possible dosages are equally probable with probability $\varepsilon_F/4$. We denote $\pi(H_t = i) = P(H_t = i|D_t^{P_1}, D_t^{P_2}, \varepsilon_F)$ after accounting for missing data and dosage error (the dependence on parental dosages is not shown).

Let ε be the error probability for the offspring dosage data and the likelihood $l_{ij}(D_t^o) = P(D_t^o|H_t = i, X_t^o = j, \varepsilon)$. For missing dosage data, we set the likelihood $l_{ij}(D_t^o) = 1$ conditional on the pattern of missing data. We assume that the observed dosage takes one of the other four possible dosages with probability 1/4, given that an error occurs. Thus, it holds that $l_{ij}(D_t^o) = 1 - \varepsilon$ if the observed dosage D_t^o is the same as the dosage value that is derived from $H_t = i$ and $X_t^o = j$ and $l_{ij}(D_t^o) = \varepsilon/4$ otherwise.

The gamete model

Bivalent chromosome pairing: A gamete is produced from a pair of bivalents in the tetraploid parent. For example, we consider the bivalent formation in parent P_1. Let the bracket $[c_1c_2]$ $(c_1 < c_2)$ denote the bivalent formed between chromosomes $c_1, c_2 = I, \ldots, IV$. After crossover between chromosomes of the bivalent $[c_1c_2]$, the resulting chromosome consists of mosaic blocks with the parental origins c_1 and c_2. We model the parental origins along the resulting chromosome as a discrete-time Markov chain. The parental origin at the first locus can be equally c_1 or c_2. The transition probability matrix is given by

$$\tau_{[c_1c_2]} = \begin{array}{c} \\ c_1 \\ c_1 \end{array} \begin{array}{c} \begin{array}{cc} c_1 & c_2 \end{array} \\ \begin{bmatrix} 1-r & r \\ r & 1-r \end{bmatrix} \end{array}$$

where r is the known recombination frequency between two loci, or it can be calculated from the genetic distance (*e.g.*, Haldane mapping function).

The crossover events are assumed to occur independently for the two bivalents when producing a diploid gamete. Thus, the discrete-time Markov chain for the parental origins along the two chromosomes can be derived easily. Let $[c_1c_2][c_3c_4]$ denote the two bivalent pairs, and it may take one of three possible combinations, [12][34], [13][24], or [14][23]. The parental origin state at the first locus can be c_1c_3, c_1c_4, c_2c_3, or c_2c_4, each with equal probability 1/4. The gamete transition matrix is given by $T_{[c_1c_2][c_3c_4]} = \tau_{[c_1c_2]} \otimes \tau_{[c_3c_4]}$, a Kronecker product between the transition matrices for the two bivalents.

Quadrivalent chromosome pairing: A gamete is produced from a multivalent in the tetraploid parent, *e.g.*, P_1. The biological meiosis process of quadrivalent pairing is very complicated, and the resulting gamete genotypes at two linked loci depend on many factors, such as the configuration of the four chromosomes and the locations of the two loci relative to the centromere (*e.g.*, Stift *et al.* 2010). We build a simple discrete-time Markov chain for the parental origins along the two

chromosomes, aiming to account for the phenomenon of double reduction resulting from quadrivalent pairing.

The parental origin process is assumed to be independent along each of the two chromosomes within the gamete produced. Along one chromosome, the parental origin state at the first locus can be 1, 2, 3, or 4, each with equal probability 1/4; the transition matrix is given by

$$\tau_{[1234]} = \begin{array}{c} \\ 1 \\ 2 \\ 3 \\ 4 \end{array} \begin{array}{c} \begin{array}{cccc} 1 & 2 & 3 & 4 \end{array} \\ \begin{bmatrix} 1-r & r/3 & r/3 & r/3 \\ r/3 & 1-r & r/3 & r/3 \\ r/3 & r/3 & 1-r & r/3 \\ r/3 & r/3 & r/3 & 1-r \end{bmatrix} \end{array}$$

so the parental origin changes into one of the other three possible values with equal probability 1/3 given that a transition occurs between the two loci with probability r. Along the two chromosomes of the diploid gamete, the parental origin state at the first locus can be one of 16 phased genotypes with equal probability, and the transition matrix is given by $T_{[1234]} = \tau_{[1234]} \otimes \tau_{[1234]}$.

Among the 16 phased genotypes, there are four with double reduction: 11, 22, 33, and 44. The prior probability of double reduction is thus 1/4, which is also the highest value given for the maximum possible double-reduction rate (Luo *et al.* 2006); values of 1/6, 1/7, and 1/8 are also mentioned (Mather 1935; Sybenga 1972; Voorrips and Maliepaard 2012). However, our prior probability will hardly affect ancestral inference when marker data are substantial.

The zygote model

The two gametes constituting a zygote are assumed to be produced independently during meiosis. Let $V_o = (V_o^{P_1}, V_o^{P_2})$, where V_o^p denotes the two bivalents or the quadrivalent formed in parent $p = P_1, P_2$ when producing offspring o. Let p_{quad} be the probability that a gamete is produced from quadrivalent formation and p_{pref} be the extra probability of pairing between homologous chromosomes with respect to that between homeologous chromosomes. Consider, *e.g.*, a P_1 gamete that is produced via bivalent formation with probability $1 - p_{quad}$, and the resulting pair of bivalents is [12][34], [13][24], and [14][23] with probabilities $p_{pref} + (1 - p_{pref})/3$, $(1 - p_{pref})/3$, and $(1 - p_{pref})/3$, respectively, assuming that [12][34] is the preferred homologous pairing. For the bvModel, we set *a priori* $p_{quad} = 0$ and $p_{pref} = 0$, so $V_o^{P_1}$ or $V_o^{P_2}$ can be equally one of the three possible bivalent pairings; for the fullModel, we set *a priori* $p_{quad} = 1/4$ and $p_{pref} = 0$, so $V_o^{P_1}$ or $V_o^{P_2}$ can be equally one of the four possible chromosome pairings.

Consider, *e.g.*, that offspring o is produced by bivalent formations in both parents, with $V_o^{P_1} = [c_1c_2][c_3c_4]$ and $V_o^{P_2} = [c_5c_6][c_7c_8]$. Along the four chromosomes of offspring o, the parental origin X_1^o at the first locus can be equally one of $N_s = 4 \times 4 = 16$ possible combinations (*e.g.*, $c_1c_3c_5c_7$). The transition matrix is given by $T^o = T_{[c_1c_2][c_3c_4]} \otimes T_{[c_5c_6][c_7c_8]}$, a Kronecker product between the gamete transition matrices.

If the P_1 gamete is produced from a quadrivalent formation, $V_o^{P_1} = [1234]$. The zygote transition matrix $T^o = T_{[1234]} \otimes T_{[c_5c_6][c_7c_8]}$ and thus the parental origin X_1^o can be equally one of $N_s = 16 \times 4 = 64$ possible states. Similarly $T^o = T_{[c_1c_2][c_3c_4]} \otimes T_{[5678]}$ for the P_2 gamete resulting from a multivalent formation, where $T_{[5678]}$ is the same as $T_{[1234]}$ except the state labels. If both gametes are produced from a quadrivalent formation, there are $N_s = 16 \times 16 = 256$ equally possible states, and $T^o = T_{[1234]} \otimes T_{[5678]}$.

Table 1 The 14 simulated scenarios classified into the three types

Type	Data set	Marker segregation type	Preferential pairing	Quadrivalent pairing
A	DStd-M	Mixed	0	0
	DPref-M	Mixed	1/2	0
	DQuad-M	Mixed	0	2/3
	DPrefQuad-M	Mixed	1/2	1/2
B	DStd-01	Nulliplex-simplex	0	0
	DStd-02	Nulliplex-duplex	0	0
	DStd-11	Simplex-simplex	0	0
	DStd-12	Simplex-duplex	0	0
	DStd-13	Simplex-triplex	0	0
	DStd-22	Duplex -duplex	0	0
C	DStd-M-V0.25	Mixed	0	0
	DStd-M-V1	Mixed	0	0
	DStd-M-Local	Mixed	0	0
	DStd-M-Long	Mixed	0	0

For the mixed-segregation type, each parental allele at a SNP site is a dosage allele with probability ½, so the expected relative proportions are 8, 6, 8, 24, 8, and 9 for the types nulliplex-simplex, nulliplex-duplex, simplex-simplex, simplex-duplex, simple-triplex, and duplex-duplex, respectively. The nulliplex-simplex refers to the unordered parental dosages 01, 03, 14, and 34 and so on for the other types. Note that the type C data sets are derived from DStd-M by disturbing the genetic map.

Parental linkage phasing

Phasing algorithm: We estimate the parental haplotype H by maximizing the marginal likelihood $\text{logl}(H) = \sum_{o=1}^{N_o} \ln P(D_o|H)$, where $P(D_o|H)$ is the marginal likelihood for offspring o with dosage data D_o. In addition, we denote by $P(V_o|D_o, H)$ the posterior probability of V_o for offspring o, which will be used in the phasing algorithm. The calculation of $P(D_o|H)$ and $P(V_o|D_o, H)$ is described in the next section on ancestral inference. The maximization is an adaptation of the Metropolis algorithm (*e.g.*, Gelman *et al.* 2004), where the acceptance always increases the target function $\text{logl}(H)$. The algorithm proceeds as follows:

A0. Sample a starting parental haplotype H. To set an overdispersed starting point, we randomly sample H_t to be one of M_t possible values compatible with the parental dosages $D_t^{P_1}$ and $D_t^{P_2}$, for $t = 1, \ldots, N_t$.

A1. Sample V_o independently for offspring $o = 1, \ldots, N_o$. Conditional on H, set V_o that maximizes the posterior probability $P(V_o|D_o, H)$ over all possible chromosome pairing values V_o.

A2. Sample a proposal H^* and $\{X_t^o\}_{t=1,\ldots,N_t}^{o=1,\ldots,N_o}$ from their posterior distribution conditional on $V = \{V_o\}_{o=1}^{N_o}$, which will be described in algorithms B and C.

A3. Calculate ratio $= e^{\text{logl}(H^*) - \text{logl}(H)}$. If ratio > 1, set $H = H^*$ and return to A1; if ratio $= 1$, stop the algorithm, and if ratio < 1, reject the proposal and return to A1.

Table 2 Estimates of parental linkage phases

	N_o = 10		N_o = 20		N_o = 100	
Data set	N_t = 75	N_t = 300	N_t = 75	N_t = 300	N_t = 75	N_t = 300
DStd-M	6 (−9.9)[a]	8 (0.0003)	0	0	0	0
DPref-M	56 (−36.7)	4 (0)	0	0	0	0
DQuad-M	40 (−4.6)	0	0	0	0	0
DPrefQuad-M	8 (−14.9)	130 (55.5)	0	0	0	0
DStd-01	0	0	0	0	0	0
DStd-02	56 (0)	160 (0)	24 (0)	184 (0)	60 (0)	144 (0)
DStd-11	70 (−104.0)	0	0	0	0	0
DStd-12	4 (0.002)	16 (0.0001)	0	0	0	0
DStd-13	0	860 (0)	0	0	196 (0)	860 (0)
DStd-22	12 (0.001)	360 (0)	68 (0)	0	68 (0)	332 (0)
DStd-M-V0.25	0	8 (−0.0003)	0	0	0	0
DStd-M-V1	54 (−70.4)	4 (0)	0	0	0	0
DStd-M-Local	128 (−75.3)	4 (0)	0	0	0	0
DStd-M-Long	106 (−34.7)	98 (483.6)	30 (17.9)	56 (361.7)	6 (100.3)	36 (114.0)

Each cell gives the number of mismatched alleles between estimated and true parental haplotypes, where the value in parentheses is the log likelihood given the estimated haplotypes minus that given the true haplotypes. For each of the 14 simulation scenarios (Table 1), six sub–data sets are specified by the number N_o = 10, 20, and 100 offspring and the number N_t = 75 and 300 markers.

[a] For example, 6 is the number of mismatched alleles out of the total $8N_t = 600$ alleles, and −9.9 is given by logl(estimate H) − logl(true H) (see the phasing algorithm).

In addition, we stop a single phasing run of algorithm A if it rejects in C_{stuck} consecutive iterations or it reaches the prefixed maximum number of iterations C_{it}. By default, we set $C_{\text{stuck}} = 10$ and $C_{\text{it}} = 100$ based on our simulation studies.

To find the global maximization, we perform multiple runs of algorithm A and select the one with the largest target function value. We repeat algorithm A until the largest logl(H) among the so-far phasing runs has been obtained C_{rep} times including the current run or the number of runs reaches the prefixed threshold C_{run}. By default, we set $C_{\text{rep}} = 3$ and $C_{\text{run}} = 20$ based on our simulation studies.

To increase computational efficiency, we exclude quadrivalent formations, so V_o can take only one of the nine possible values. As shown in the simulated studies, the phasing algorithm is very robust to the quadrivalent inheritance.

Proposal sampling: To sample the parental haplotypes, we first extend the forward algorithm (Rabiner 1989) to calculate the marginal posterior probabilities of latent H_t and $\{X_t^o\}_{o=1}^{N_o}$ at locus t, integrating out the previous parental haplotypes $\{H_t\}_{t'=1}^{t-1}$ and parental origins $\{X_{t'}^o\}_{t'=1,\ldots,t-1}^{o=1,\ldots,N_o}$. Denote by $\Omega_t = \{D_t^o, D_{t'}^{p_1}, D_{t'}^{p_2}\}_{t'=1}^{t}$ the dosage data up to locus t. For offspring o, we denote by $\tilde{\alpha}_{ij}^o(t) = P(\Omega_t, X_t^o = j | H_t = i, V)$ and $\alpha_{ij}^o(t) = P(X_t^o = j | H_t = i, \Omega_t, V)$, where $\alpha_{ij}^o(t) = \tilde{\alpha}_{ij}^o(t) / \sum_{j=1}^{N_s} \tilde{\alpha}_{ij}^o(t)$ according to the Bayesian theorem (Gelman *et al.* 2004). We denote by $\tilde{p}_i(t) = P(\Omega_t, H_t = i | V)$ and $p_i(t) = P(H_t = i | \Omega_t, V)$, where $p_i(t) = \tilde{p}_i(t) / \sum_{i=1}^{M_t} \tilde{p}_i(t)$ according to the Bayesian theorem (Gelman *et al.* 2004). The algorithm proceeds as follows:

B0. Initialize $\tilde{\alpha}_{ij}^o(1) = l_{ij}(D_1^o)\pi_j^o$, for $o = 1, \ldots, N_o$, $i = 1, \ldots, M_1$, and $j = 1, \ldots, N_s$. Then calculate $\tilde{p}_i(1) = \pi(H_1 = i) \prod_{o=1}^{N_o} \sum_{j=1}^{N_s} \tilde{\alpha}_{ij}^o(1)$. Remember that π_j^o is the initial distribution for the discrete-time Markov chain of offspring o and that $\pi(H_t = i)$ is used as the prior haplotype probability after accounting for the missing data and errors in parental dosages. We obtain $\alpha_{ij}^o(1)$ and $p_i(1)$ by normalizing $\tilde{\alpha}_{ij}^o(1)$ and $\tilde{p}_i(1)$, respectively.

B1. For $t = 2, \ldots, N_t$, compute

$$\tilde{\alpha}_{ij}^o(t) = \sum_{i'=1}^{M_{t-1}} \sum_{j'=1}^{N_s} \tilde{p}_{i'}(t-1) \alpha_{i'j'}^o(t-1) T_{j'j}^o(t-1) l_{ij}(D_t^o) \quad \textit{and}$$

$$\tilde{p}_i(t) = \pi(H_t = i) \prod_{o=1}^{N_o} \sum_{j=1}^{N_s} \tilde{\alpha}_{ij}^o(t)$$

We obtain $\alpha_{ij}^o(t)$ and $p_i(t)$ by normalizing $\tilde{\alpha}_{ij}^o(t)$ and $\tilde{p}_i(t)$, respectively.

Based on the probabilities $\alpha_{ij}^o(t)$ and $p_i(t)$ calculated forwardly by algorithm B, we sample the parental haplotypes and the parental origins backwardly:

C0. Sample $H_{N_t} = i$ from $p_i(N_t)(i = 1, \ldots, M_{N_t})$; sample $X_{N_t}^o = j$ from $\alpha_{ij}^o(N_t)(j = 1, \ldots, N_s)$ independently for $o = 1, \ldots, N_o$, conditional on the haplotype $H_{N_t} = i$.

C1. For $t = N_t - 1, \ldots, 1$,

i. Conditional on $X_{t+1}^o = j'$, compute $\tilde{\beta}_{ij}^o(t) = \alpha_{ij}^o(t) T_{jj'}^o(t)$ and $\tilde{q}_i(t) = p_i(t) \prod_{o=1}^{N_o} \sum_{j=1}^{N_s} \tilde{\beta}_{ij}^o(t)$.

ii. Sample $H_t = i$ from the unnormalized probabilities $\tilde{q}_i(t)(i = 1, \ldots, M_t)$.

iii. Conditional on $H_t = i$, sample $X_t^o = j$ from the unnormalized probabilities $\tilde{\beta}_{ij}^o(t)(j = 1, \ldots, N_s)$ independently for $o = 1, \ldots, N_o$.

Ancestral inference

Let H be the parental haplotype estimated by the phasing algorithm A or any given parental haplotype. Denote by D_o

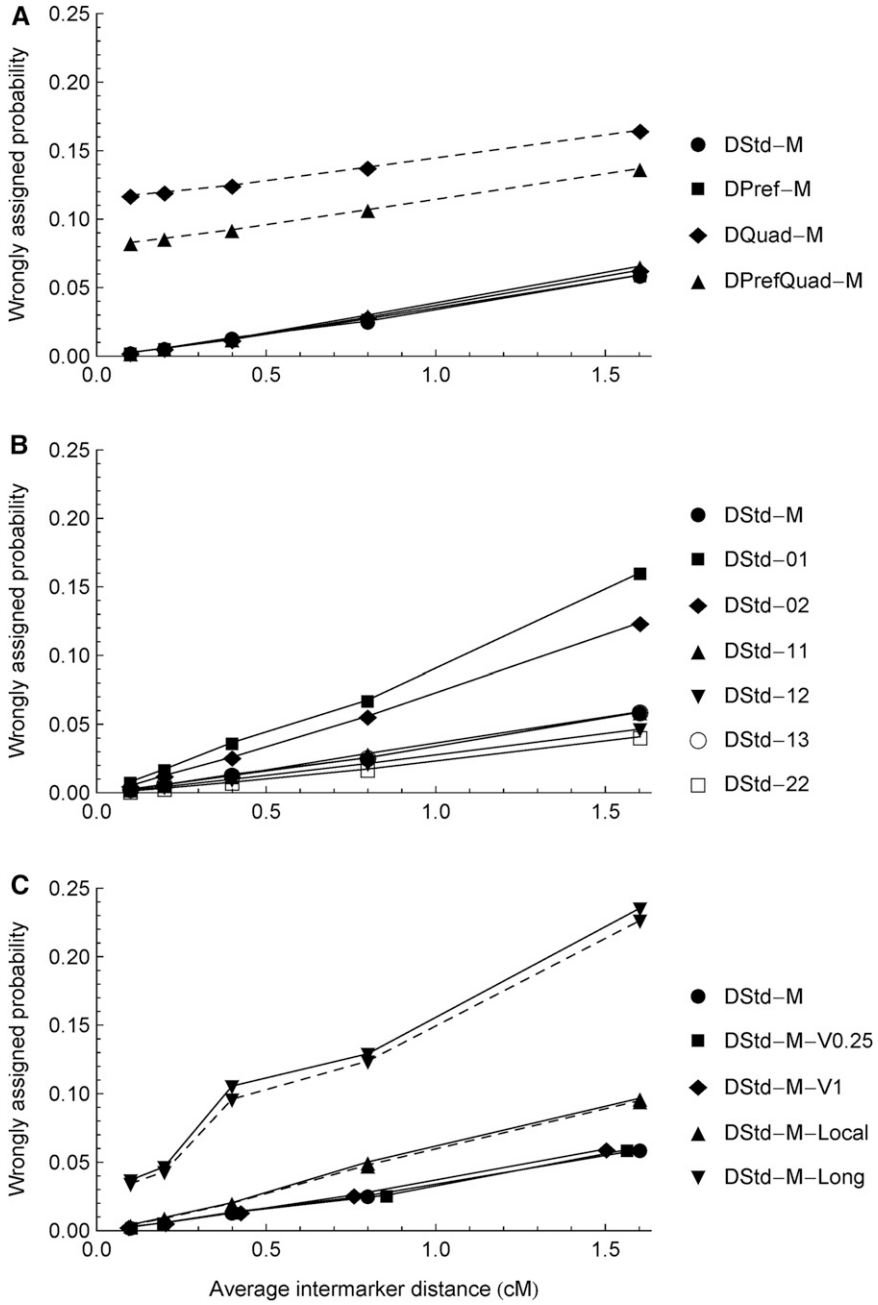

Figure 2 Density dependencies of ancestral inference for the three types of the 14 simulation scenarios (Table 1). The *y*-axis is the wrongly assigned probability, one minus the posterior probability of being the true ancestral state, averaged over the N_o = 200 offspring and all markers. The increasing intermarker distances correspond to the numbers of markers N_T = 1200, 600, 300, 150, and 75 on a 120-cM chromosome, respectively. The symbols connected by the solid lines denote the results obtained from the fullModel and the dashed lines from the bvModel. Except for DQuad-M, DPref-Quad-M, DStd-M-Local, and DStd-M-Long, the results from the bvModel and the fullModel are the same because all the offspring are identified as being produced only by bivalent pairing in the full-Model. In B, the results for DStd-11 and DStd-13 largely overlap with those for DStd-M.

the dosage data for offspring o. For each of the 9 (bvModel) or 16 (fullModel) possible values of V_o, we calculate the marginal likelihood $P(D_o|H,V_o)$ and the posterior probability $P(X_t^o|D_o,H,V_o)$ by integrating out the latent parental origins $\{X_t^o\}_{t=1}^{N_t}$ using the forward-backward algorithm (Rabiner 1989) independently for $o = 1,\ldots,N_o$.

We divide offspring into four possible types, 22, 24, 42, and 44, where the first digit denotes the bivalent (digit 2) or quadrivalent (digit 4) formation in parent P_1, and the second digit, for parent P_2. We set each offspring to the type with the largest probability. For example, the posterior probability $P[\text{type}(o) = 22|D_o,H]$ of offspring o being type 22 can be obtained by summing the posterior probability $P(V_o = k|D_o,H)$ over 9 of the 16 possible values for bivalent pairing. The posterior probability of the chromosome pairing V_o is given by

$$P(V_o|D_o,H) = \frac{P(D_o|H,V_o)P(V_0|H)}{P(D_o|H)}$$

where $P(D_o|H) = \sum_{V_o} P(D_o|H,V_o)P(V_0|H)$ according to the law of total probability. Here the prior probability $P(V_0|H)$ is assumed to be independent of parental haplotype H, and it is determined by the preferential probability p_{pref} and the quadrivalent probability p_{quad}. We have $P(V_0|H) = 1/9$ for the bvModel and $1/16$ for the fullModel.

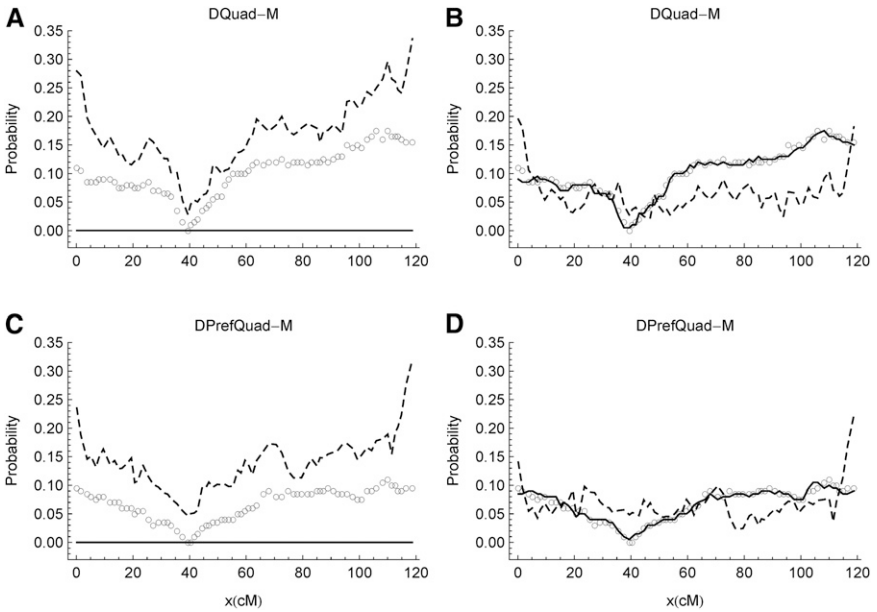

Figure 3 Estimation of double reduction along the chromosomes obtained from DQuad-M (top panels) and DPrefQuad-M (bottom panels). Each data set has N_O = 200 offspring and N_t = 75 markers. The left panels are from the bvModel, and the right panels are from the fullModel. The solid lines denote the estimations, the posterior probabilities of double-reduction states averaged over the offspring at a given marker; the empty circles denote the true values, the fractions of offspring being in double-reduction states. The dashed lines denote the wrongly assigned probabilities along the chromosomes, one minus the posterior probability of being the true ancestral state, averaged over all offspring but not markers.

After assigning the chromosome pairing type for each offspring, we obtain the final marginal posterior probability

$$P\left[X_t^o \middle| D_o, H, type(o)\right] = \frac{\sum_k P\left(X_t^o \middle| D_o, H, V_o = k\right) P(V_o = k | D_o, H)}{P[type(o) | D_o, H]}$$

where the summation is taken over all the possible chromosome pairing values that are compatible with the assigned type. Note that the possible ancestral origin states depend on V_o during the weighted summation.

Data availability

The TetraOrigin package has been implemented in Mathematica 9.0 (Wolfram Research 2012) and is freely available under the GNU General Public License from the website https://github.com/chaozhi/TetraOrigin.git. The full data sets for the 14 simulation scenarios and the real potato data extracted from Hackett *et al.* (2013) are included in the package.

Results

Simulation experiments

We evaluate the performance and robustness of our method on haplotype reconstruction by intensive simulation studies in full-sib tetraploid families. We simulate 14 scenarios using PedigreeSim v2.0 (Voorrips and Maliepaard 2012), differing with respect to preferential and/or quadrivalent pairing, marker segregation type, and accuracy of genetic maps (Table 1). We simulate only one linkage group. The full data set of each scenario consists of 200 offspring and 1200 SNPs randomly distributed along four homologous/homeologous chromosomes of 120 cM in length; the centromere is located at 40 cM.

The 14 scenarios can be divided into three types. Type A has different combinations of preferential and quadrivalent pairings. We denote by DStd-M the standard data set without preferential pairing and without quadrivalent pairing, where -M refers to the mixed segregation types owing to mixed parental dosages. Type B has six scenarios with the data sets denoted by DStd-*st*, where the segregation type *st* = 01, 02, 11, 12, 13, or 22 refers to the unordered dosages of two parents at each SNP locus; the segregations with the parental dosages 03, 14, 23, 24, 33, and 34 are equivalent to one of the preceding segregation types by switching dosage alleles into nondosage alleles for parents and offspring (see Table 1). Type C has four scenarios for studying sensitivity to erroneous genetic maps, and they are derived from DStd-M by disturbing the intermarker distances or the marker ordering while keeping the dosages unchanged. We denote by -V0.25 (-V1) the disturbance of intermarker distances by a gamma distribution with mean being the original distance and variance being 0.25 (1), by -Local the disturbance of marker ordering by partitioning chromosomes into segments of 10 consecutive markers and swapping two markers within each segment, and by -Long for each of the 10 pairs of markers being chosen randomly within the same linkage group (not necessarily within the same segment). We consider only one linkage group for each simulation scenario and perform the disturbances independently for each sub–data set.

We carry out multilocus haplotype reconstruction for each of the 14 scenarios using the network model illustrated in Figure 1 and described in detail in the *Methods* section. The haplotype reconstruction is divided into two stages: parental linkage phasing and ancestral inference. For each stage, two models can be used: bvModel, where only preferential or nonpreferential bivalent pairings are modeled, and fullModel, where both bivalent and quadrivalent pairings are modeled. We evaluate separately the results obtained from each stage. In addition, we study the impact of missing data by analyzing DStd-M with a given fraction of dosages regarded as missing and the effects of dosage errors based on data sets derived

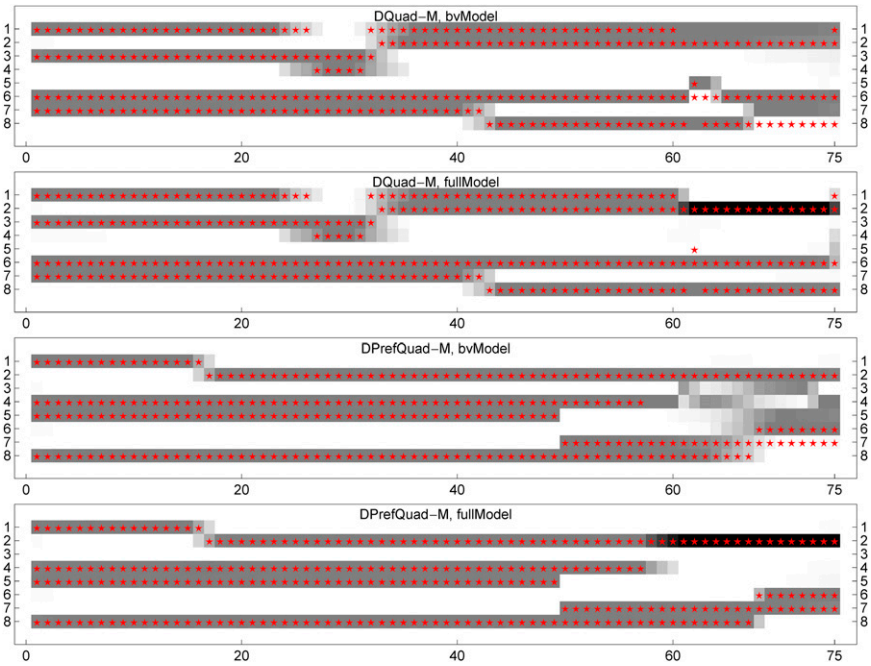

Figure 4 The posterior haplotype probabilities for two typical offspring. The top two panels show the results obtained from DQuad-M using the bvModel and the fullModel, respectively; the bottom two panels, for the offspring from DPrefQuad-M. The *x*-axis refers to the N_t = 75 SNP markers, and the *y*-axis refers to the eight parental chromosomal origins of two parents. The red stars denote the true ancestral origins, and the gray levels denote the haplotype probabilities, with white = 0 and black =0.5; the haplotype probabilities at each marker sum to 1. The black bands indicate the double reduction where two copies of alleles have the same parental origin.

from DStd-M by changing the correct dosage to another random dosage in a specified fraction of data points.

Evaluation of parental linkage phasing

To test the effect of sample size, for each full data set, we extract six nested subsets with the number of offspring N_o = 10, 20, and 100 and the number of markers N_t = 75 and 300 obtained by sampling every sixteenth and fourth of the 1200 markers, respectively. For each subset, we perform phasing analysis using the bvModel because the fullModel is more computationally intensive. Because the permutation of the four haplotypes within each parent is arbitrary and nonidentifiable from dosage data, we label the ordering of the most probable parental haplotypes obtained from the simulated data sets so that the number of mismatches with their true (simulated) values is minimized and keep the same labeling for real data where the true values are not known. Table 2 shows the comparisons of estimated parental haplotypes with their true values.

We first examine the phasing results for the sample sizes N_o = 20 and 100. For the type A scenarios, the estimated parental haplotypes match the true values, despite the presence of preferential and/or quadrivalent pairings. For the type B scenarios, most of the estimations match the true values, except for some segregation types such as *st* = 02, 13, and 22 (Table 2). We may obtain different mismatches if we repeat the phasing analysis with random starting values, but these estimations are always equivalent to their true values in terms of marginal likelihood (Table 2). The mismatches are shown in Supplemental Material, Figure S1, where the dosage and nondosage alleles are switched at some markers for segregation type *st* = 02, but there is no clear pattern for *st* = 13 or 22. For each of the type B scenarios, we repeated the phasing analysis at least twice, and the segregation types *st* = 01, 11, and 12 did not show such equivalent mismatches. For the type C scenarios, the phasing analyses are robust to the noise of intermarker distances and the local disturbance of marker ordering but not to long-range disturbances. In the latter case, the marginal likelihoods for the estimated parental haplotypes are larger than those for the true values, indicating that the phasing analysis cannot be improved without jointly re-estimating the marker ordering (Table 2).

For the smallest sample size N_o = 10, the parental phasing varies with repeated analysis and thus is unreliable. This inconsistency of results may occur because many similar haplotypes are indistinguishable based on the small data sets; the phasing results are improved with higher marker density, as shown by the larger likelihood values. However, there is no visible effect of marker density for the larger sample sizes N_o = 20 and 100.

Furthermore, we evaluate the effect of missing data on parental linkage phasing by using DStd-M with N_o = 200 and N_t = 300. Dosages are assumed to be missing at random. We perform phasing analysis for the missing fraction among two parents being 0, 0.1, 0.2, 0.5, 0.75, and 1 and the missing fraction among offspring being 0, 0.1, 0.2, 0.5, and 0.75. For all 30 combinations of missing fractions, we successfully recover the true parental haplotypes.

Evaluation of ancestral inference

For each simulated data set, we perform ancestral inference (*i.e.*, for each progeny individual we obtain its genetic composition in terms of parental homolog segments) and compare this to their true compositions. To study the effects of marker density, for each of the 14 full data sets we extract sub–data sets by sampling every *i*th marker for i = 1, 2, 4, 8, and 16 such that the marker subsets are nested and recursively reduced by half; the average intermarker distance of 0.1 cM for the full data set is doubled repeatedly until we reach 1.6 cM for the smallest sub–data set.

Figure 2 shows the effects of marker density on the wrongly assigned probability for each of the 14 full data sets. The wrongly assigned probability is given by one minus the posterior probability of being the true ancestral state, averaged over all markers and offspring. As expected, the wrongly assigned probabilities increase roughly linearly with the average intermarker distances. Figure 2A shows that the effects of density from the fullModel (solid lines) depend little on the chromosome pairings; the wrongly assigned probabilities from DQuad-M and DPrefQuad-M using the bvModel (dashed lines) are larger than those using the fullModel, and the excess amounts approximate the average double-reduction probabilities (Figure 3). Figure 2B shows that segregation types 01 and 02 are less informative for ancestral inference than other types.

Figure 2C shows the sensitivities of ancestral inference to an erroneous genetic linkage map. The noises of intermarker distances have little effect on the wrongly assigned probabilities. The local disturbances of marker ordering almost double the wrongly assigned probabilities, though they do not affect the parental linkage phasing (Table 2). The long-distance disturbances have the greatest deleterious effects on ancestral inference because they also deteriorate the phasing accuracy (Table 2). For both the local and long-distance disturbances of marker ordering, the wrongly assigned probabilities obtained from the fullModel are slightly larger than those from the bvModel, probably because for some offspring quadrivalents are wrongly assigned (Figure S2).

Figure 3 shows the estimations of double reduction along chromosomes obtained from DQuad-M and DPrefQuad-M using both the bvModel and the fullModel. For both data sets, the true double-reduction probabilities are zero at the centromere and increase toward the telomeres. Because the bvModel does not allow double reduction, the wrongly assigned probabilities along chromosomes are positively correlated with the true double-reduction fractions (Figure 3, A and B). In contrast, the fullModel estimates the double reduction very well, and thus the wrongly assigned probabilities are small and uncorrelated with the true double-reduction fractions along chromosomes (Figure 3, C and D); the wrongly assigned probabilities are relatively large at the chromosomal ends because the marker information is available only from one side.

Figure 4 shows the posterior haplotype probabilities along the chromosomes for two offspring, one from each of DQuad-M and DPrefQuad-M. The haplotype probability refers to the probability of each allele at a locus being one of the eight parental origins of the two parents. The gradual changes of gray levels around the recombination breakpoints indicate the large uncertainties of identifying the true ancestral states there. Both the bvModel and the fullModel estimate the parental origins very well in the chromosomal region without double reduction. The fullModel successfully identifies the true double-reduction states on the right end of chromosomes (Figure 4), while the bvModel identifies parental origins correctly for only two or three of four alleles at a locus. Figure S2 shows similar results from the posterior genotype probabilities along the chromosomes.

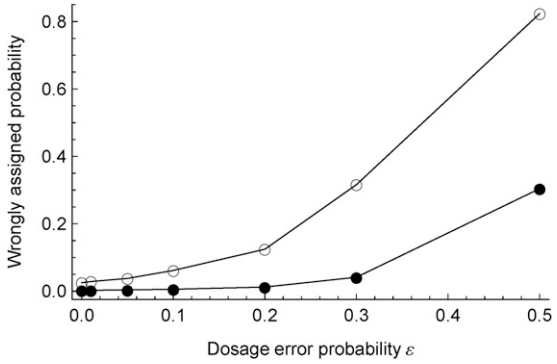

Figure 5 Effect of offspring dosage error on ancestral inference, conditional on true parental linkage phases. The filled (open) circles refer to the derived DStd-M with the number N_o = 200 offspring and the number N_t = 1200 (N_t = 50) SNP markers.

Effects of dosage errors

To evaluate the effects of dosage errors, we analyze the data sets derived from DStd-M by combining two marker densities $N_t = 150$ and 1200 and seven dosage error probabilities $\varepsilon = 0$, 0.01, 0.05, 0.1, 0.2, 0.3, and 0.5. All the $N_o = 200$ offspring are included. Each derived data set is obtained by applying errors to offspring dosages using the dosage error model described in the *Methods* section. We do not apply errors on parental dosages partly because of the intensive computational load but mainly because these errors might be detectable in real data based on offspring dosages. We use the true dosage error probabilities and the bvModel in the following phasing analysis and ancestral inference.

Table S1 shows the results of the estimated parental linkage phases. The true parental haplotypes are successfully recovered from the sparse marker data sets with $\varepsilon \leq 0.2$ and from the dense marker data sets with $\varepsilon \leq 0.3$. For the data sets with large dosage error probability, the phasing algorithm failed to find the global maximization when the number of phasing runs reached the default threshold $C_{run} = 20$.

Figure 5 shows the effects of offspring dosage errors on ancestral inference conditional on true parental haplotypes. The wrongly assigned probability increases nonlinearly with the offspring dosage error probability: the dosage errors have very little effect on ancestral inference for the data sets with dosage error probability less than ~0.2.

Comparisons using simulated data

We compare the performance of TetraOrigin with H2013 (Hackett *et al.* 2013) using the simulated data sets. For H2013, the parental linkage phasing involves heuristic algorithms for placing nonsimplex markers with respect to the phased framework of simplex markers (segregation type 01) and subsequent manual assignment for the remaining markers. Because only a few simplex markers are available for small simulated data sets and extensive manual work is required for large data sets, we perform the comparisons on ancestral inference but not on parental linkage phasing.

Table 3 shows the comparisons of ancestral inferences conditional on the true parental haplotypes, where H2013 cannot

Table 3 Comparisons of ancestral inference between TetraOrigin and H2013 for the 14 simulation scenarios (Table 1)

	N_o = 100, N_t = 75			N_o = 100, N_t = 300		
Data set	TetraOrigin (bvModel)	TetraOrigin (fullModel)	H2013	TetraOrigin (bvModel)	TetraOrigin (fullModel)	H2013
DStd-M	0.061	0.061	0.144	0.015	0.015	0.023
DPref-M	0.060	0.060	0.136	0.014	0.014	0.022
DQuad-M	0.164	0.062	N/A	0.122	0.012	N/A
DPrefQuad-M	0.146	0.065	N/A	0.101	0.013	N/A
DStd-01	0.157	0.157	0.329	0.038	0.038	0.053
DStd-02	0.126	0.126	0.222	0.027	0.027	0.036
DStd-11	0.059	0.059	0.149	0.013	0.013	0.022
DStd-12	0.043	0.043	0.114	0.011	0.011	0.018
DStd-13	0.060	0.060	0.158	0.014	0.014	0.023
DStd-22	0.042	0.043	0.098	0.008	0.008	0.016
DStd-M-V0.25	0.064	0.064	0.148	0.014	0.014	0.021
DStd-M-V1	0.067	0.067	0.155	0.015	0.015	0.025
DStd-M-Local	0.100	0.101	0.171	0.020	0.020	0.026
DStd-M-Long	0.222	0.229	0.287	0.097	0.107	0.066

For each scenario, two sub–data sets are specified by the number N_o = 100 offspring and the number N_t = 75 or 300 markers. Each cell gives the wrongly assigned probability conditional on the true parental haplotypes. The DQuad-M and DPrefQuad-M data sets could not be analyzed with H2013.

be applied to DQuad-M and DPrefQuad-M. Except for DStd-M-Long, the wrongly assigned probabilities for the sparse marker data ($N_t = 75$) using H2013 are around two times larger than those using TetraOrigin and 1.5 times larger than the dense marker data ($N_t = 300$). As shown in Table S2, the differences become smaller when the estimations are compared in terms of the wrongly *called* probability. Here the wrongly called probability is given by one minus the fraction of the calls being the true states, where the calls are determined by the ancestral states with the maximum posterior probabilities. Consistently, Figure S3 shows that the posterior genotype probabilities along the chromosomes obtained from H2013 are noisier than those from TetraOrigin.

Table 3 and Table S2 indicate that TetraOrigin extracts more information from marker data than H2013. As a result, for DStd-M-Long, TetraOrigin performs generally a bit worse than H2013, indicating that TetraOrigin is more sensitive to the long-range disturbances of marker ordering.

Comparisons using real potato data

We evaluate TetraOrigin by using real SNP dosage data from potato (Hackett *et al.* 2013) for a comparison of results with H2013. For the potato mapping population of parents and 190 offspring, 1093 of the 5378 polymorphic SNPs are assigned to the constructed genetic map of 12 chromosomes (Hackett *et al.* 2013). We set the dosage error probability to be 0.01 for the dosage data, assuming no dosage error for the two parents. We analyze each chromosome (linkage group) independently.

Table 4 shows the comparisons for each of the 12 chromosomes between TetraOrigin (bvModel) and H2013. The parental haplotypes estimated by the two methods are the same for seven chromosomes, and for the other chromosomes, there are a few mismatches mainly around the telomeres (Figure S4). The haplotypes estimated by TetraOrigin are strongly supported in terms of marginal likelihood (Table 4).

We perform ancestral inference by TetraOrigin (bvModel) and H2013, conditional on their estimated parental haplotypes. We call the ancestral states at all the markers for each offspring by their maximum posterior probabilities and calculate the fraction of consistent calls between the two methods. As shown in Table 4, on average, 86% of the calls are consistent, while, of course, the true ancestral states are unknown.

Figure 6 (A–C) shows the genome-wide posterior genotype probabilities for a typical offspring obtained by H2013 and TetraOrigin (bvModel and fullModel). Consistent with the simulation studies (Figure S3), the results from H2013 are noisier than those from TetraOrigin. For example, the ancestral states around 600 cM (chromosome *VII*) and 980 cM (chromosome *XI*) are more likely to be identified unambiguously in TetraOrigin. The results from TetraOrigin (fullModel) are different from those from TetraOrigin (bvModel) only for chromosomes *I*, *III*, and *IV* (Figure 6C). The results from TetraOrigin (fullModel) indicate double-reduction segments on the right ends of chromosomes *I* and *III*, while the tiny double-reduction segment around the middle of chromosome *IV* (~330 cM) is likely to be artifactual.

Figure 6D shows the maximum posterior genotype probabilities along the chromosomes averaged over the 190 offspring. The probabilities obtained from TetraOrigin are much larger than those from H2013. TetraOrigin (fullModel) indicates that the average double-reduction probability is around 0.04, larger than the estimate based only on a subset of markers of a different potato mapping population (Bourke *et al.* 2015). As expected, double reduction occurs more frequently at the telomeres than near the centromere (Figure 6D).

Discussion

We have developed a novel statistical framework for multilocus haplotype reconstruction in outcrossing tetraploids from SNP dosage data, where the two-stage implementation of

Table 4 Comparisons between TetraOrigin (bvModel) and H2013 obtained from the real potato data

Chromosome:	*I*	*II*	*III*	*IV*	*V*	*VI*	*VII*	*VIII*	*IX*	*X*	*XI*	*XII*
No. of SNPs:	142	120	74	152	119	122	89	85	91	104	85	118
No. of mismatches[a]:	0	0	6	0	0	0	0	0	6	12	6	4
Δlogl[b]:	0	0	164.4	0	0	0	0	0	21.4	1248.4	227.7	309.3
Consistency[c]:	0.91	0.91	0.84	0.88	0.93	0.88	0.91	0.90	0.72	0.86	0.70	0.92

[a] The number of mismatches between the parental haplotypes estimated from TetraOrigin and those from H2013.
[b] The log likelihood given the TetraOrigin estimated parental haplotypes minus that given the H2013 estimated parental haplotypes.
[c] The fraction of ancestral states called by their maximum posterior probabilities that are consistent between two methods.

parental linkage phasing and ancestral inference is built on an integrated network model of tetraploid inheritance in TetraOrigin. Simulation studies demonstrate that the new haplotype reconstruction is robust to preferential bivalent and quadrivalent pairing during meiosis, to the six marker segregation types, to erroneous genetic maps (except in the case of long-range disturbances in marker ordering), and to the various fractions of missing data in parents and offspring dosages.

We have compared the performance of TetraOrigin and the methodology described in Hackett *et al.* (2013), H2013. For ancestral inference, H2013 cannot be applied to data sets with quadrivalent pairings, and otherwise, the results are noisier than those from TetraOrigin. For parental linkage phasing, H2013 uses a heuristic multilocus algorithm and requires manual manipulation of intermediate results, and thus, it is less accurate and more time-consuming than TetraOrigin, which uses a fully probabilistic multilocus algorithm (Table 4). In addition, the algorithm for phase reconstruction by H2013 starts from a framework of simplex SNPs and thus has potential difficulties in analyzing data sets with a limited number of simplex SNPs, although this has not been a problem in practice (C. Hackett, personal communication).

Modeling quadrivalent pairing has been a theoretically challenging topic in quantitative genetics, and most studies have been built on the pioneering work of Fisher (1947) and Mather (1936). Fisher (1947) proposed a conceptual two-locus tetrasomic model where all 136 gamete genotypes are classified into 11 modes of gamete formation according to the occurrence of double-reduction and recombination events between two loci. Luo *et al.* (2004) established a deterministic relationship between the coefficient of double reduction at two linked loci and the recombination fraction between them, which subsequently has been applied to two- and multilocus linkage analysis (Luo *et al.* 2006; Leach *et al.* 2010).

In contrast to Leach *et al.* (2010), we have built a simpler model of quadrivalent pairing, assuming that the ancestral origins along a chromosome follow a time-homogeneous Markov chain independently between two homologous (homeologous) chromosomes of a diploid gamete. Remarkably, our nonmechanistic model produces very good estimations of double reduction (Figure 3), indicating that the marker data (200 offspring and 75 markers within the linkage group) provide enough information on double reduction. Also, the accurate estimation may be due to the equivalence between the transition probability matrix of gamete genotypes in our model and that derived by Leach *et al.* (2010) based on the 136 two-locus gamete genotypes, although the transition in our model refers to the 16 phased (ordered) genotypes from one locus to the next, instead of the 10 unphased genotypes in Leach *et al.* (2010).

The simulation studies show that the haplotype reconstruction is not sensitive to intermarker distances, indicating that the assumption of no genetic interference is not critical and that improving the accuracy of the intermarker distances by multilocus linkage analysis may be of marginal value to haplotype reconstruction and thus to QTL mapping. We have also assumed implicitly that there is no selection and thus no segregation distortion. This assumption is used as a prior in TetraOrigin, and the calculated posterior probabilities of parental origins may contain segregation distortion information passed from marker data when parent and offspring dosages are known in distortion regions. However, if parental dosage information is missing in regions with distorted segregation, that might result in incorrect estimation of parental origin and QTL mapping.

TetraOrigin is very capable of handling missing data and dosage errors in parents and offspring. However, accounting for possible dosage errors in parents results in a more than 10-fold reduction in the computational speed of parental linkage phasing because the total number of phases over all the possible dosages per locus increases dramatically. For example, for DStd-M with 200 offspring and 300 markers, the running times on a standard desktop are around 10 and 144 min for the missing fractions of parental dosages being 0 and 1, respectively, assuming no parental dosage error. When accounting for parental dosage error, the running time for the missing fraction 0 of parental dosages would be similar to that for the missing fraction 1. Thus, it is advantageous to perform quality control of parental dosages based on offspring dosages. Accounting for dosage error in the offspring imposes no such computational cost, and error rates of up to 20% in sparse data sets and 30% in dense data sets are handled well (Figure 5). This flexibility may be pertinent to genotyping-by-sequencing data; in particular, relatively low genome coverage typically results in higher error frequency.

The nulliplex-simplex and nulliplex-duplex segregation types are the least informative for ancestral inference, yet these markers, along with simplex-simplex markers, have been used most commonly in mapping studies. If this is the case here, a

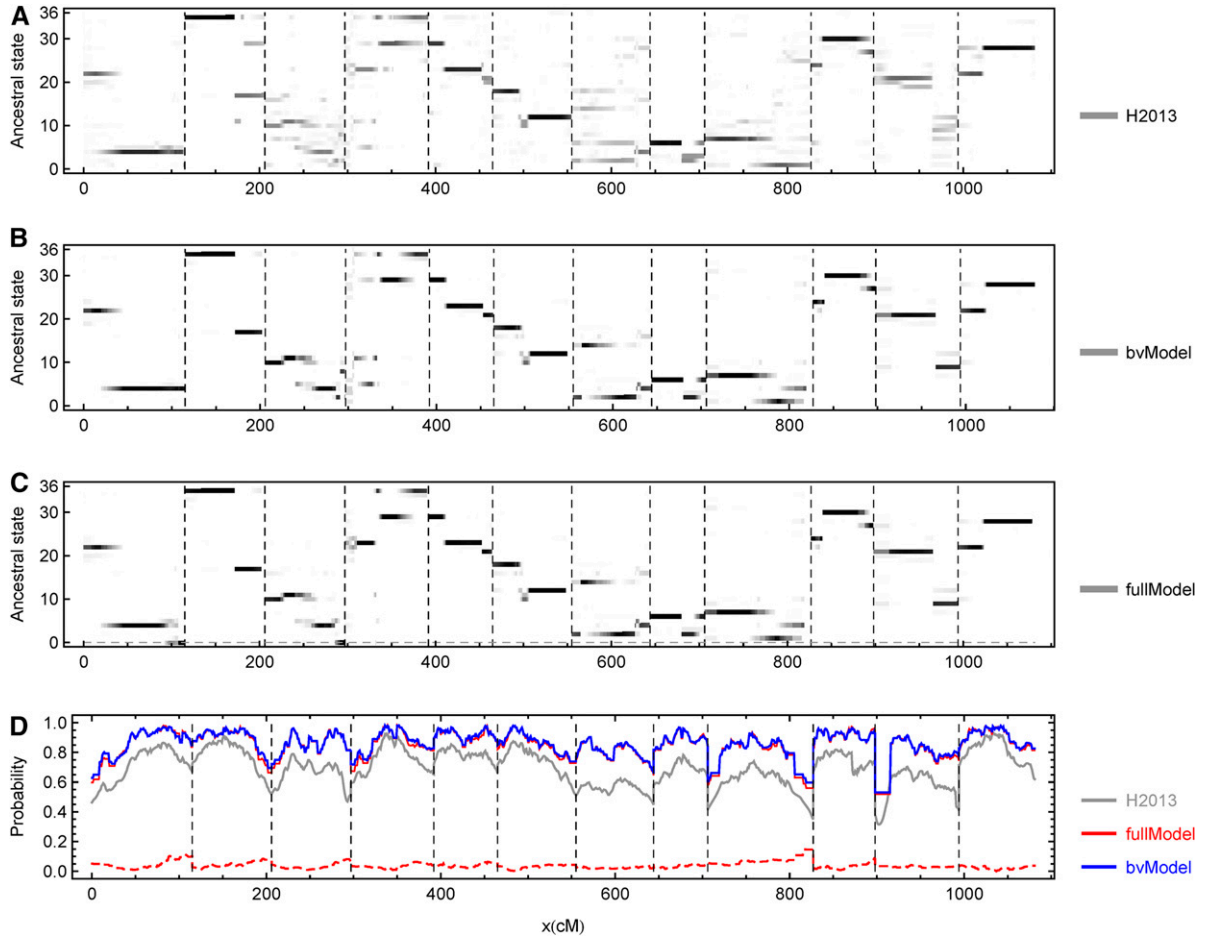

Figure 6 Evaluation of ancestral inference along each chromosome obtained from the real potato data set. The dashed vertical lines indicate the chromosomal boundaries. (A–C) The posterior genotype probabilities for an offspring obtained from H2013, TetraOrigin (bvModel), and TetraOrigin (fullModel), respectively. The probabilities are represented by the gray levels, with white = 0 and black = 1. The dashed horizontal line in C denotes the collapsed genotypes with double reduction in the fullModel. (D) The maximum posterior probabilities averaged over the 190 offspring. The gray, blue, and red lines refer to the results obtained from H2013, TetraOrigin (bvModel), and TetraOrigin (fullModel), respectively; the results from the bvModel and fullModel overlap. The red dashed line denotes the estimated double-reduction probabilities by the fullModel.

lack of informative markers on the genetic map may limit the accuracy of estimation by our proposed method. However, if a genome sequence is available, the unmapped markers still may be roughly positioned. More important, current approaches in tetraploid species use most or all marker types (Hackett *et al.* 2013).

The network model can, in principle, be applied to higher, even-ploidy levels, but we would need to improve the phasing algorithm for computational efficiency. For example, the number of possible bivalent pairings in a tetraploid parent is 3, which increases to 15 for hexaploids and to 105 for octoploids. Thus, the number of combinations of bivalent pairings in two parents increases from 3^2 for tetraploids, to 15^2 for hexaploids, and to 105^2 for octoploids. As a result, we cannot simply perform the maximization step with respect to all the possible combinations of bivalent pairings, at least for octoploid or higher polyploid species. At the tetraploid level, the rigorous framework of TetraOrigin yields accurate posterior genotype probabilities that are needed for downstream QTL analysis in outcrossing tetraploids, even in the absence of parental dosage information.

Acknowledgments

We acknowledge Peter Bourke and Fred A. van Eeuwijk for their helpful comments. R.E.V. and J.J. acknowledge financial support from the TKI polyploids project, "A genetic analysis pipeline for polyploid crops" (project number BO-26.03-002-001). Work by C.A.H. was supported by the Scottish government's Rural and Environment Science and Analytical Services Division (RESAS).

Author contributions: J.H. and M.C.A.M.B. initiated and conceived the study. C.Z. and M.C.A.M.B. designed the experiments. C.Z. developed the models and the algorithms, implemented the TetraOrigin software, and performed the analyses using TetraOrigin. R.E.V., J.J., and M.C.A.M.B. contributed to model development. R.E.V. generated the simulated data sets using PedigreeSim software.

C.A.H. performed the ranalyses using the H2013 method. C.Z. wrote the first draft of the manuscript, and R.E.V., C.A.H., J.H., and M.C.A.M.B. contributed substantially to revisions. The authors declare no conflicts of interest.

Literature Cited

Bourke, P. M., R. E. Voorrips, R. G. F. Visser, and C. Maliepaard, 2015 The double reduction landscape in tetraploid potato as revealed by a high-density linkage map. Genetics 201: 853–863.

Broman, K. W., H. Wu, S. Sen, and G. A. Churchill, 2003 R/qtl: Qtl mapping in experimental crosses. Bioinformatics 19: 889–890.

Fisher, R. A., 1947 The theory of linkage in polysomic inheritance. Philos. Trans. R. Soc. Lond. B Biol. Sci. 233: 55–87.

Garcia, A. A. F., M. Mollinari, T. G. Marconi, O. R. Serang, R. R. Silva *et al.*, 2013 Snp genotyping allows an in-depth characterisation of the genome of sugarcane and other complex autopolyploids. Sci. Rep. 3: 3399.

Gelman, A., J. Carlin, H. Stern, and D. Rubin, 2004 *Bayesian Data Analysis*. Chapman & Hall/CRC, Boca Raton, FL.

Hackett, C. A., J. E. Bradshaw, and J. W. McNicol, 2001 Interval mapping of quantitative trait loci in autotetraploid species. Genetics 159: 1819–1832.

Hackett, C. A., K. McLean, and G. J. Bryan, 2013 Linkage analysis and qtl mapping using snp dosage data in a tetraploid potato mapping population. PLoS One 8: e63939.

Leach, L. J., L. Wang, M. J. Kearsey, and Z. W. Luo, 2010 Multilocus tetrasomic linkage analysis using hidden Markov chain model. Proc. Natl. Acad. Sci. USA 107: 4270–4274.

Li, X., Y. Wei, A. Acharya, Q. Jiang, J. Kang *et al.*, 2014 A saturated genetic linkage map of autotetraploid alfalfa (Medicago sativa L.) developed using genotyping-by-sequencing is highly syntenous with the Medicago truncatula genome. G3 4: 1971–1979.

Liu, E. Y., Q. Zhang, L. McMillan, F. Pardo-Manuel de Villena, and W. Wang, 2010 Efficient genome ancestry inference in complex pedigrees with inbreeding. Bioinformatics 26: i199–i207.

Luo, Z. W., C. A. Hackett, J. E. Bradshaw, J. W. McNicol, and D. Milbourne, 2001 Construction of a genetic linkage map in tetraploid species using molecular markers. Genetics 157: 1369–1385.

Luo, Z. W., R. M. Zhang, and M. J. Kearsey, 2004 Theoretical basis for genetic linkage analysis in autotetraploid species. Proc. Natl. Acad. Sci. USA 101: 7040–7045.

Luo, Z. W., Z. Zhang, L. Leach, R. M. Zhang, J. E. Bradshaw *et al.*, 2006 Constructing genetic linkage maps under a tetrasomic model. Genetics 172: 2635–2645.

Mather, K., 1935 Reductional and equational separation of the chromosomes in bivalents and multivalents. J. Genet. 30: 53–78.

Mather, K., 1936 Segregation and linkage in autotetraploids. J. Genet. 32: 287–314.

Mott, R., C. J. Talbot, M. G. Turri, A. C. Collins, and J. Flint, 2000 A method for fine mapping quantitative trait loci in outbred animal stocks. Proc. Natl. Acad. Sci. USA 97: 12649–12654.

Rabiner, L., 1989 A tutorial on hidden Markov models and selected applications in speech recognition. Proc. IEEE 77: 257–286.

Stam, P., 1993 Construction of integrated genetic-linkage maps by means of a new computer package—joinmap. Plant J. 3: 739–744.

Stift, M., R. Reeve, and P. H. van Tienderen, 2010 Inheritance in tetraploid yeast revisited: segregation patterns and statistical power under different inheritance models. J. Evol. Biol. 23: 1570–1578.

Sybenga, J., 1972 *General cytogenetics*. North-Holland, Amsterdam.

Sybenga, J., 1994 Preferential pairing estimates from multivalent frequencies in tetraploids. Genome 37: 1045–1055.

Voorrips, R. E., and C. A. Maliepaard, 2012 The simulation of meiosis in diploid and tetraploid organisms using various genetic models. BMC Bioinformatics 13: 248.

Voorrips, R. E., G. Gort, and B. Vosman, 2011 Genotype calling in tetraploid species from bi-allelic marker data using mixture models. BMC Bioinformatics 12: 172.

Wolfram Research, 2012 Mathematica, v9.0 edn. Wolfram Research, Inc., Champaign, IL.

Xie, C. G., and S. H. Xu, 2000 Mapping quantitative trait loci in tetraploid populations. Genet. Res. 76: 105–115.

Zheng, C. Z., M. P. Boer, and F. A. van Eeuwijk, 2015 Reconstruction of genome ancestry blocks in multiparental populations. Genetics 200: 1073–1087.

Communicating editor: G. A. Churchill

GENETICS

Supporting Information
www.genetics.org/lookup/suppl/doi:10.1534/genetics.115.185579/-/DC1

Probabilistic Multilocus Haplotype Reconstruction in Outcrossing Tetraploids

Chaozhi Zheng, Roeland E. Voorrips, Johannes Jansen, Christine A. Hackett, Julie Ho, and Marco C. A. M. Bink

DOI: 10.1534/genetics.115.185579

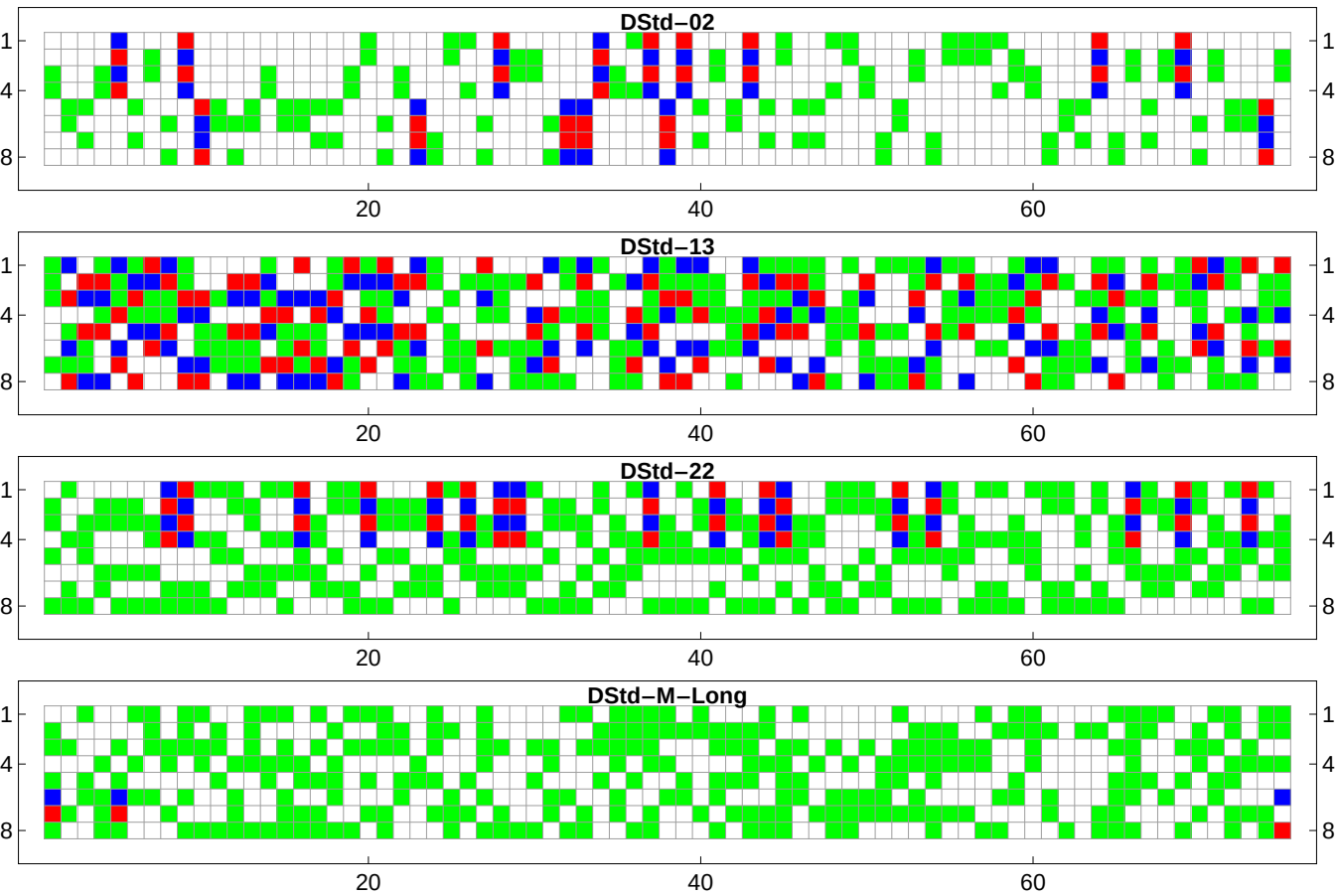
DStd−02
DStd−13
DStd−22
DStd−M−Long
1
4
8
20
40
60

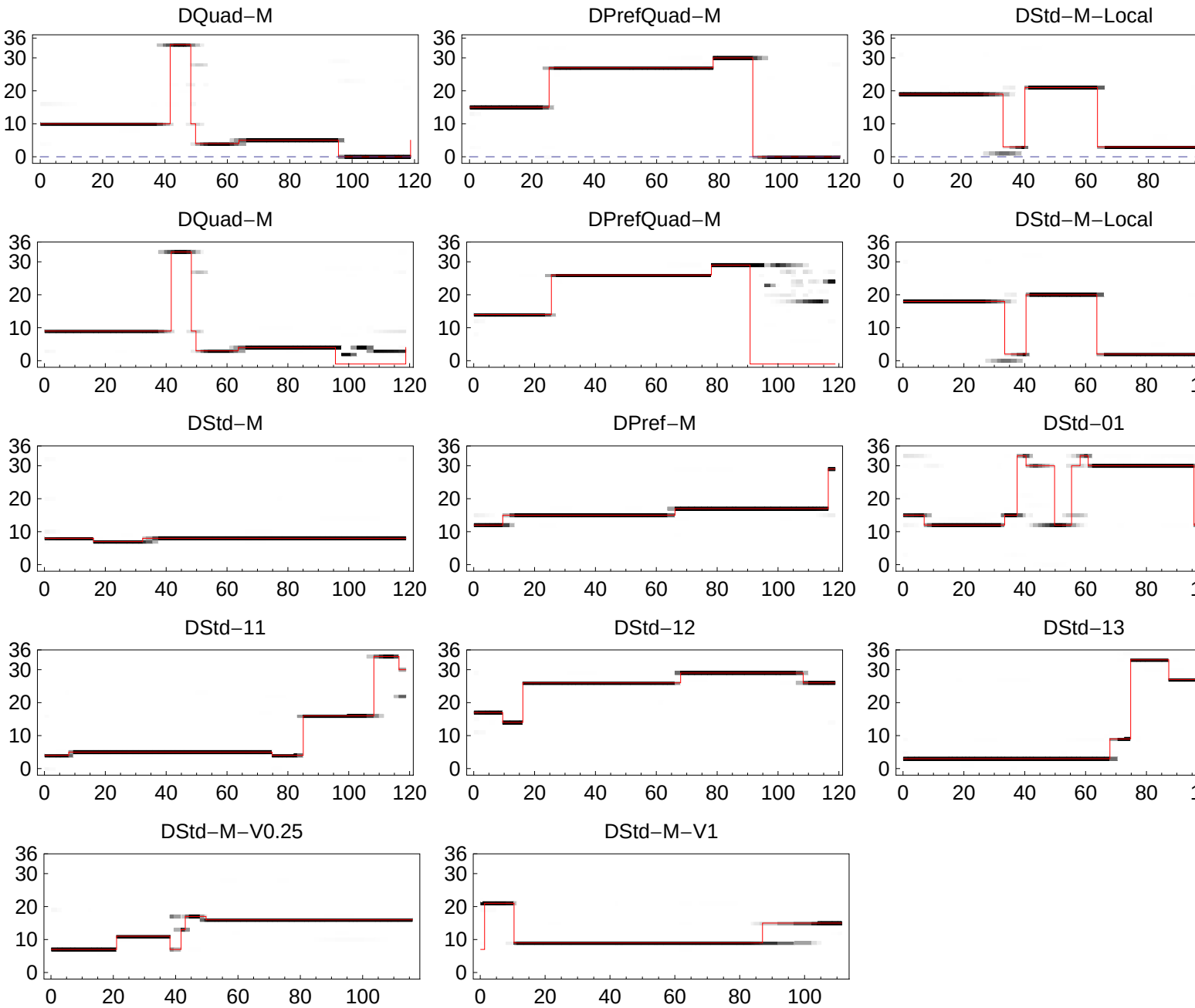
DQuad−M
DPrefQuad−M
DStd−M−Local
DQuad−M
DPrefQuad−M
DStd−M−Local
DStd−M
DPref−M
DStd−01
DStd−11
DStd−12
DStd−13
DStd−M−V0.25
DStd−M−V1

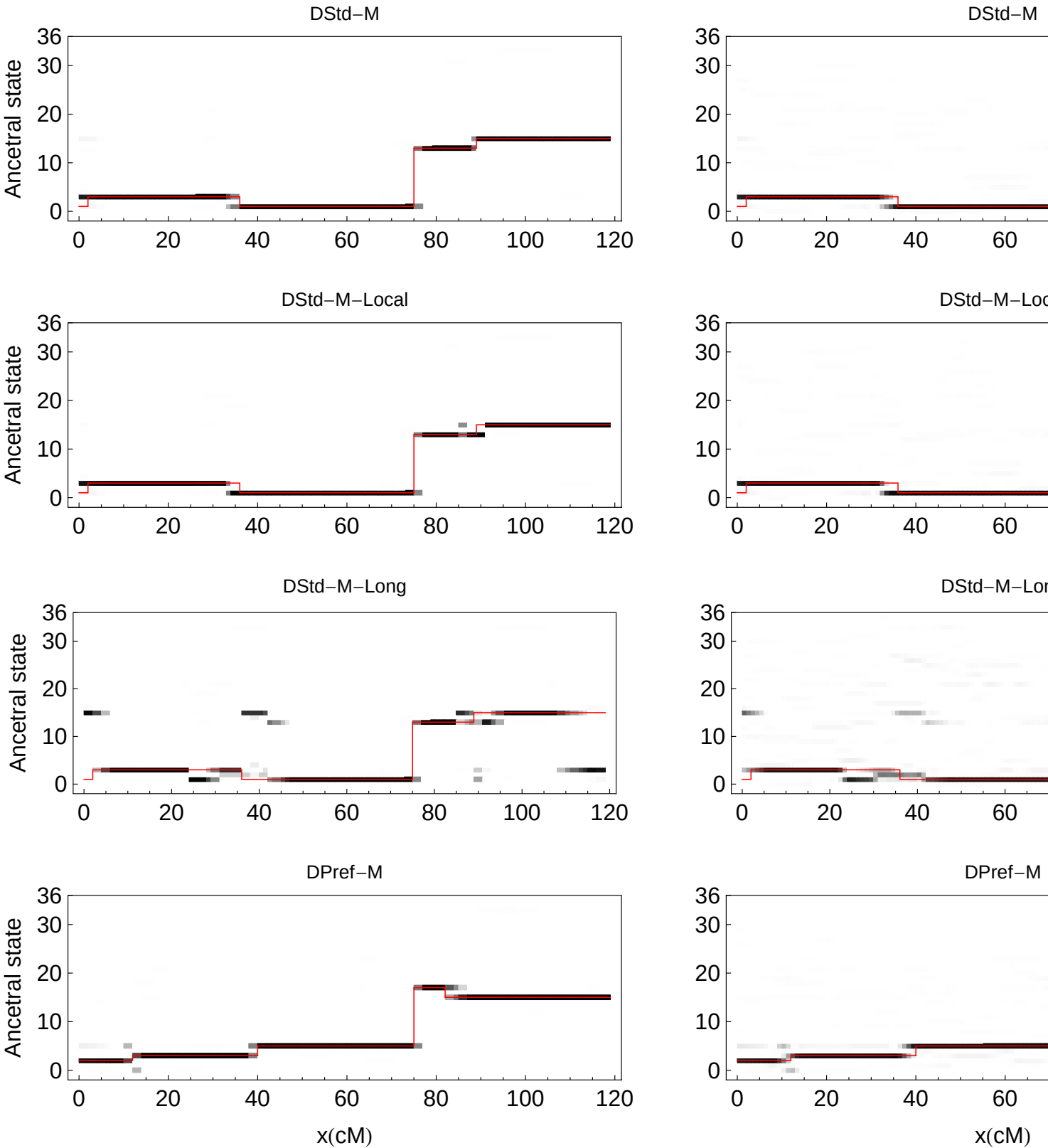
DStd−M
DStd−M−Local
DStd−M−Long
DPref−M
Ancetral state
x(cM)
0
10
20
30
36
0
20
40
60
80
100
120

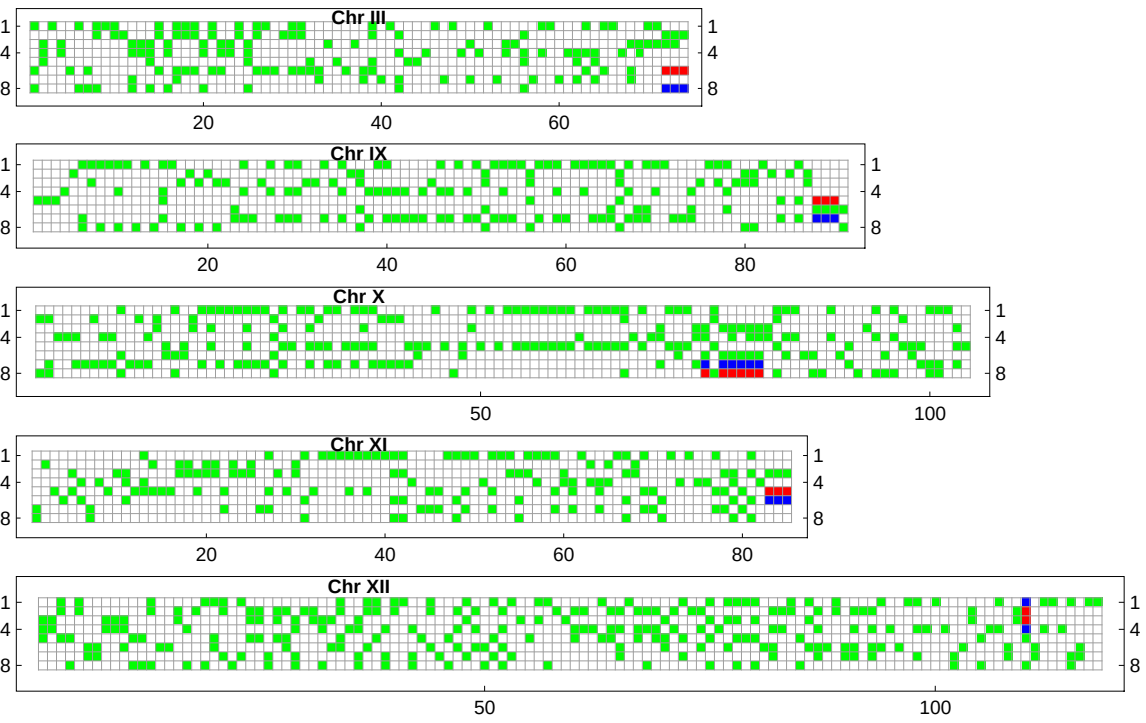
Chr III
1
4
8
20
40
60
Chr IX
80
Chr X
50
100
Chr XI
Chr XII

Table S1 Similar to Table 3 but each cell gives the wrongly called probability instead of the wrongly assigned probability.

Dataset	$N_O = 100, N_T = 75$			$N_O = 100, N_T = 300$		
	TetraOrigin (bvModel)	TetraOrigin (fullModel)	H2013	TetraOrigin (bvModel)	TetraOrigin (fullModel)	H2013
DStd-M	0.044	0.044	0.059	0.012	0.012	0.017
DPref-M	0.045	0.045	0.059	0.012	0.012	0.016
DQuad-M	0.150	0.046	N/A	0.120	0.009	N/A
DPrefQuad-M	0.131	0.048	N/A	0.098	0.010	N/A
DStd-01	0.110	0.110	0.124	0.028	0.028	0.033
DStd-02	0.092	0.092	0.108	0.020	0.020	0.024
DStd-11	0.043	0.043	0.059	0.010	0.010	0.016
DStd-12	0.031	0.031	0.047	0.008	0.008	0.015
DStd-13	0.044	0.044	0.061	0.010	0.010	0.017
DStd-22	0.034	0.034	0.053	0.007	0.007	0.013
DStd-M-V0.25	0.049	0.049	0.066	0.011	0.011	0.014
DStd-M-V1	0.054	0.054	0.075	0.013	0.013	0.018
DStd-M-Local	0.081	0.083	0.082	0.016	0.016	0.020
DStd-M-Long	0.200	0.205	0.166	0.067	0.081	0.054

Table S2 Estimations of parental linkage phases for DStd-M after applying various amounts of errors on offspring dosages. Each cell gives the number of mismatched alleles between estimated and true parental haplotypes, where the value in parentheses is the log likelihood given the estimated haplotypes minus that given the true haplotypes. The sparse (or dense) datasets are specified by the number $N_O = 200$ of offspring and the number $N_T = 150$ (or 1200) of markers.

Dosage error probability ε	$\mathrm{N_O} = 200, \mathrm{N_T} = 150$	$\mathrm{N_O} = 200, \mathrm{N_T} = 1200$
0	0	0
0.01	0	0
0.05	0	0
0.1	0	0
0.2	0	0
0.3	78 (-992.11)	0
0.5	426 (-79.04)	3456 (-3575.14)